

WISCA: A Lightweight Model Transition Method to Improve LLM Training via Weight Scaling

Jiacheng Li^{1,2*}, Jianchao Tan^{1*}, Zhidong Yang^{2,3}, Pingwei Sun¹, Feiye Huo¹, Jiayu Qin¹, Yerui Sun¹, Yuchen Xie¹, Xunliang Cai¹, Xiangyu Zhang², Maoxin He⁴, Guangming Tan², Weile Jia², Tong Zhao^{2†},

¹Meituan, Beijing, China

²State Key Lab of Processors, Institute of Computing Technology, Chinese Academy of Sciences, Beijing, China

³Hong Kong University of Science and Technology, Hong Kong SAR, China

⁴Xiamen University, Xiamen, China

{ljiacheng14,tanjianchao02,sunpingwei,huofeiye,qinjiayu02,sunyerui,caixunliang}@meituan.com,
{zhaotong,jiaweile,yangzhidong19s,zhangxiangyu22z,tgm}@ict.ac.cn, hmx@xmu.edu.cn

Abstract

Transformer architecture gradually dominates the LLM field. Recent advances in training optimization for Transformer-based large language models (LLMs) primarily focus on architectural modifications or optimizer adjustments. However, these approaches lack systematic optimization of weight patterns during training. Weight pattern refers to the distribution and relative magnitudes of weight parameters in a neural network. To address this issue, we propose a Weight Scaling method called WISCA to enhance training efficiency and model quality by strategically improving neural network weight patterns—without changing network structures. By rescaling weights while preserving model outputs, WISCA indirectly optimizes the model’s training trajectory. Experiments demonstrate that WISCA significantly improves convergence quality (measured by generalization capability and loss reduction), particularly in LLMs with Grouped Query Attention (GQA) architectures and LoRA fine-tuning tasks. Empirical results show **5.6%** average improvement on zero-shot validation tasks and **2.12%** average reduction in training perplexity across multiple architectures.

Introduction

The weight pattern is defined as the arrangement and scaling of parameters across layers in a neural network, which plays a pivotal role in the convergence of neural networks. For example, although a two-layer fully connected network theoretically can approximate any function (universal approximation theorem) (Barron 1993), its performance on complex tasks is often suboptimal due to poorly structured weight patterns. In contrast, modern architectures (e.g., CNNs, GNNs, RNNs, Transformers) achieve superior results by implicitly optimizing weight patterns for specific tasks. These architectures reduce optimization complexity and enhance representational capability through structured designs (e.g., local receptive fields in CNNs (LeCun et al. 2002), attention mechanisms in Transformers (Vaswani et al. 2017)), demon-

*These authors contributed equally.

†Corresponding author.

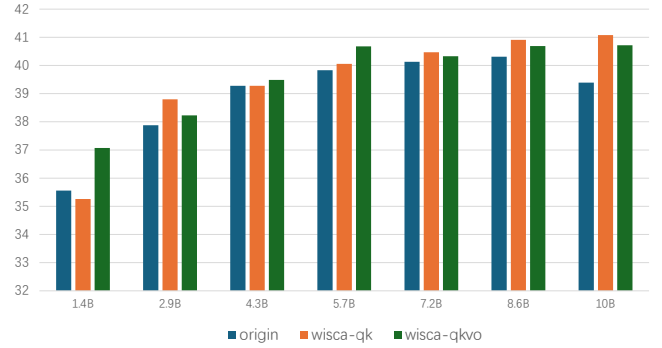


Figure 1: The comparisons of average zero-shot evaluation results at different training steps using WISCA and original methods on llama-moe-5B-A0.8B. All metrics can be seen in Appendix.

strating that an effective weight pattern is a key factor in their success.

A typical example of a poor weight pattern in a neural network that leads to suboptimal model performance is the sharp minimum problem. As demonstrated in (Keskar et al. 2016), training with excessively large batch sizes increases the likelihood of converging to sharp minima. Models trapped in sharp minima exhibit significantly worse generalization on test datasets compared to those in flat minima. This discrepancy arises from the bias between the training and test sets: Firstly, the loss landscapes computed on training and test datasets diverge significantly due to their distributional differences. Secondly, because of the distributional relationship between the two datasets being close, the losses of them exhibit relatively similar but inconsistent trends in parameter spaces. The loss landscape curves of them are parallel but non-overlapping trajectories. Thus, the side impact of sharp minima on generalization is apparent. It amplifies sensitivity to outliers in the dataset and weakens the model’s robustness as a result.

In non-convex optimization, rugged convergence paths, characterized by sharp minima and highly curved regions in

the loss landscape, pose significant challenges to gradient-based optimization. Such paths force the optimizer to wander through narrow valleys and saddle points, leading to premature convergence to suboptimal solutions with poor generalization (e.g., sharp minima). In contrast, a smooth, flat convergence path allows the gradients to guide parameters in approaching a wider minimum, where small perturbations in the weights have minimal side-impact on the loss. This stability inherently improves generalization, as models in flat regions are less sensitive to outliers in the dataset. This difference highlights the critical role of loss landscape geometry in successfully converging to a wider minimum.

From the perspective of optimizing weight patterns to improve neural network training trajectories in the loss landscape and the results of convergence, we propose the Equivalent Model Theory and an optimization strategy for weight patterns (WISCA). Equivalent Model Theory gives the definition of equivalent models. Consider two models; if they have the same architecture and derive the same output with the same input despite the differences in weight configurations of them. Such two models can be regarded as equivalent models. During training, models can transition to equivalent models during training, and the training process will continue. WISCA introduces a systematic strategy to guide such transitions to superior weight patterns, thereby indirectly reshaping the training process dynamically. By prioritizing weight configurations that align with smoother optimization landscapes, WISCA enhances the likelihood of converging to a flat minimum with superior generalization performance.

Our contributions can be summarized as follows:

- We propose the Equivalent Model Theory, which establishes a theoretical foundation for enhancing model training performance through weight pattern optimization.
- Based on the proposed theory, we propose a novel model transition strategy called WISCA, which enables Transformer-based models and LoRA architectures to dynamically adjust their weight patterns to more optimal configurations during training while remaining equivalent to the unadjusted model.
- Extensive experimental results show that our WISCA can improve model performance through dynamically adjusting weights by finding equivalent models.

Theory

Sharp Minima leads to Worse Generalization

Theorem 0.1 (Generalization Gap of Sharp vs. Flat Minima). *Let θ_1 and θ_2 be two models with identical training loss $L_{train}(\theta_1) = L_{train}(\theta_2) = L_0$. If θ_1 resides in a sharp minimum (defined as $\exists \mathcal{N}(\epsilon)$, for $\forall \epsilon \in \mathcal{N}(\epsilon)$, where $\|\epsilon\| \rightarrow 0$, $L(\theta_1 + \epsilon) - L(\theta_1) > L(\theta_2 + \epsilon) - L(\theta_2)$), then the expected validation loss satisfies:*

$$\mathbb{E}[L_{val}(\theta_1)] > \mathbb{E}[L_{val}(\theta_2)]. \quad (1)$$

Proof. The proof proceeds in five steps:

Taylor Expansion of Loss Landscape: For a small perturbation $\epsilon \in \mathbb{R}^d$, the loss at $\theta + \epsilon$ is approximated by:

$$L(\theta + \epsilon) \approx L(\theta) + \frac{1}{2} \epsilon^\top H(\theta) \epsilon, \quad (2)$$

where $H(\theta) = \nabla^2 L(\theta)$ is the Hessian matrix. At minima ($\nabla L(\theta) = 0$), the first-order term vanishes.

Sharpness Characterization: The sharpness condition implies that for all ϵ :

$$\epsilon^\top H(\theta_1) \epsilon > \epsilon^\top H(\theta_2) \epsilon \Rightarrow H(\theta_1) \succeq H(\theta_2), \quad (3)$$

where \succeq denotes the positive semi-definite ordering.

Modeling Validation Loss: Assume validation data introduces a Gaussian perturbation $\delta \sim \mathcal{N}(0, \sigma^2 I)$ to the parameters. The validation loss is approximated as:

$$L_{val}(\theta) \approx L_0 + \frac{1}{2} \delta^\top H(\theta) \delta. \quad (4)$$

Expectation Calculation: Taking expectation over δ :

$$\mathbb{E}[L_{val}(\theta)] = L_0 + \frac{\sigma^2}{2} \text{Tr}(H(\theta)), \quad (5)$$

where $\text{Tr}(H(\theta))$ is the trace of the Hessian.

Inequality Derivation: Since $H(\theta_1) \succeq H(\theta_2)$, it follows that $\text{Tr}(H(\theta_1)) \geq \text{Tr}(H(\theta_2))$. Thus:

$$\begin{aligned} \mathbb{E}[L_{val}(\theta_1)] - \mathbb{E}[L_{val}(\theta_2)] &= \frac{\sigma^2}{2} (\text{Tr}(H(\theta_1)) - \text{Tr}(H(\theta_2))) \\ &> 0. \end{aligned} \quad (6)$$

□

Equivalent Model

Definition 0.2 (Equivalent Models). Let \mathcal{F} denote a neural network architecture subject to parameter space Θ , input space \mathcal{X} , and output space \mathcal{Y} . Two parameter configurations $\theta_1, \theta_2 \in \Theta$ are called **equivalent models** if they satisfy:

1. **Architectural Consistency:** θ_1 and θ_2 belong to the same architecture \mathcal{F} .
2. **Functional Equivalence:** For all inputs $\mathbf{x} \in \mathcal{X}$,

$$F(\mathbf{x}; \theta_1) = F(\mathbf{x}; \theta_2), \quad (7)$$

where $F(\cdot; \theta)$ denotes the function of forward propagation for architecture \mathcal{F} with parameters θ .

3. **Parameter Distinction:** $\theta_1 \neq \theta_2$ (i.e., their weight patterns differ).

Equivalent models represent distinct points in the parameter space Θ that map to the same functional behavior in the output space \mathcal{Y} . This concept enables optimization strategies (e.g., our proposed WISCA) to transition between equivalent models during training, effectively reshaping weight patterns without altering functional outputs.

For example, consider a two-layer fully connected network where:

1. Layer l uses $\text{ReLU}(\cdot)$ activation with zero bias,
2. Parameters are $(\mathbf{w}^{(l)}, \mathbf{w}^{(l+1)})$ and $(\alpha \mathbf{w}^{(l)}, \alpha^{-1} \mathbf{w}^{(l+1)})$

for $\alpha > 0$.

For any input \mathbf{x} , the outputs are:

$$\theta_1: \mathbf{w}^{(l+1)} \text{ReLU}(\mathbf{w}^{(l)} \mathbf{x}), \quad (8)$$

$$\theta_2: \alpha^{-1} \mathbf{w}^{(l+1)} \text{ReLU}(\alpha \mathbf{w}^{(l)} \mathbf{x}). \quad (9)$$

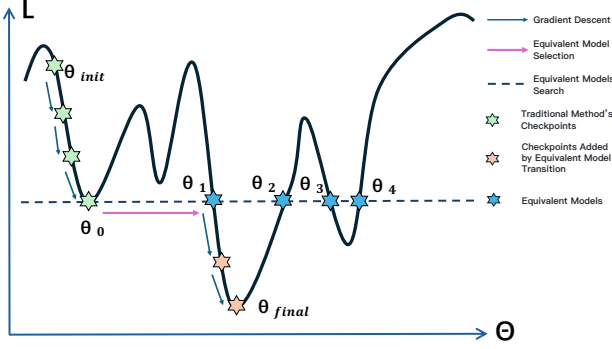


Figure 2: **Optimization via Equivalent Model Transition.** In the ideal case, the global optimum θ_{final} can be achieved through this strategy. Key notations: θ_{init} (initialized model), θ_0 (final checkpoint under conventional optimization), $\theta_1, \dots, \theta_n$ (all equivalent models explored globally), θ_{final} (global optimum). After identifying equivalent models, the optimal candidate (e.g., θ_1) is selected for continued training based on convergence potential. Theoretically, convergence to θ_{final} is guaranteed if all equivalent models are evaluable.

Since $\text{ReLU}(\alpha \mathbf{z}) = \alpha \text{ReLU}(\mathbf{z})$ for $\alpha > 0$, θ_2 simplifies to:

$$\alpha^{-1} \mathbf{w}^{(l+1)} \cdot \alpha \text{ReLU}(\mathbf{w}^{(l)} \mathbf{x}) = \mathbf{w}^{(l+1)} \text{ReLU}(\mathbf{w}^{(l)} \mathbf{x}),$$

which matches θ_1 exactly.

Thus, θ_1 and θ_2 are **equivalent models** (Definition 0.2):

- Identical architecture and outputs for all inputs,
- Distinct weight patterns ($\mathbf{w}^{(l)} \neq \alpha \mathbf{w}^{(l)}$).

An ideal implementation of the equivalent model strategy for optimizing neural network training trajectories consists of the following steps:

Escape from Local Minima: When a first-order optimizer (e.g., SGD, Adam) becomes trapped in a sharp local minimum θ_0 with poor generalization, systematically explore the set of equivalent models $[\theta_1, \theta_2, \dots, \theta_n]$ (as defined in Definition 0.2).

Model Selection: From the candidate set $[\theta_1, \theta_2, \dots, \theta_n]$, select a model θ_k that lies in a "flatter" region of the loss landscape, since such regions are empirically linked to better generalization.

Training Transition: Resume training from θ_k instead of θ_0 , leveraging the functional equivalence of the models to maintain task performance while improving optimization dynamics.

Theoretically, if one can identify all equivalent model strategies for a neural network architecture, the model can converge to the global optimum. However, it is quite challenging to implement in practice. We propose a strategy named WISCA, model transition during training that identifies partial equivalent models, which have demonstrated outstanding performance in extensive experiments.

WISCA

For an input sequence $\mathbf{X} \in \mathbb{R}^{n \times d_{\text{model}}}$ with n tokens and d_{model} -dimensional embeddings, the self-attention operation

is formulated as follows:

$$(\mathbf{Q}, \mathbf{K}, \mathbf{V}) = \mathbf{X} (\mathbf{W}_q, \mathbf{W}_k, \mathbf{W}_v) \quad (10)$$

$$\text{Att}(\mathbf{Q}, \mathbf{K}, \mathbf{V}) = \text{softmax} \left(\frac{\mathbf{Q} \mathbf{K}^\top}{\sqrt{d_k}} \right) \mathbf{V} \quad (11)$$

$$\text{Output} = \text{Att}(\mathbf{Q}, \mathbf{K}, \mathbf{V}) \mathbf{W}_o \quad (12)$$

For the θ -component ($\theta = \{W_q, W_k\}$), we model its loss landscape as:

$$\mathcal{L}(\mathbf{Q}, \mathbf{K}) = (\mathbf{Q} \mathbf{K} - C)^2, \quad C \in \mathbb{R}^+. \quad (13)$$

where, C represents the ideal value of $\mathbf{Q} \mathbf{K}$ (e.g., $C = 1$ for normalized attention).

Under the assumption of perfect equivalent model strategies, parameters can traverse *any point* on the contour lines of $\mathcal{L}(\mathbf{Q}, \mathbf{K}) = \text{const}$ (Figure 3). On the contour lines of the loss landscape, the region where $\mathbf{Q} = \mathbf{K}$ exhibits the flattest geometry. This is reflected in the top-down contour lines, where the distance between adjacent contour lines reaches the maximum when $\mathbf{Q} = \mathbf{K}$.

We assume that flatter regions of the loss landscape are of higher quality than sharper, more rugged regions at the same loss level. This superiority manifests not only in generalization performance but also in the efficiency of continued training. The core idea of WISCA is to adjust the \mathbf{Q} and \mathbf{K} values by scaling in Transformer-based architectures to satisfy $\mathbf{Q} = \mathbf{K}$ while preserving the $\mathbf{Q} \mathbf{K}^\top$ product.

As illustrated in Figure 3, WISCA modifies the initialization by enforcing $\mathbf{Q} = \mathbf{K}$, leading to fundamentally different optimization dynamics compared to random initialization. SGD-M-WISCA exhibits smoother and more stable convergence, avoiding sharp minima with WISCA-adjusted initialization.

WISCA can be applied not only during initialization but also at any iteration of the training process. Since the WISCA-adjusted model remains functionally equivalent to the original model (Definition 0.2), training can seamlessly resume from the transformed parameters.

Next, we will introduce the proposed WISCA in detail. The design of WISCA starts with vanilla self-attention in Transformer. To ensure similarity between \mathbf{Q} and \mathbf{K} while preserving the $\mathbf{Q} \mathbf{K}^\top$ product, we devise the following adjustment for W_q and W_k in WISCA:

$$W'_q = W_q \cdot \sqrt{\frac{\|W_k\|_1}{\|W_q\|_1}}, \quad (14)$$

$$W'_k = W_k \cdot \sqrt{\frac{\|W_q\|_1}{\|W_k\|_1}}, \quad (15)$$

where $\|\cdot\|_1$ denotes the L_1 -norm of a matrix (sum of absolute values of its elements).

Why does the convergence become stable after using WISCA? Here is an intuitive explanation. Considering the landscape $f(Q, K) = (QK - 1)^2$ and the current checkpoint is (Q, K) , the gradient is $2(QK - 1)(K, Q)$. After

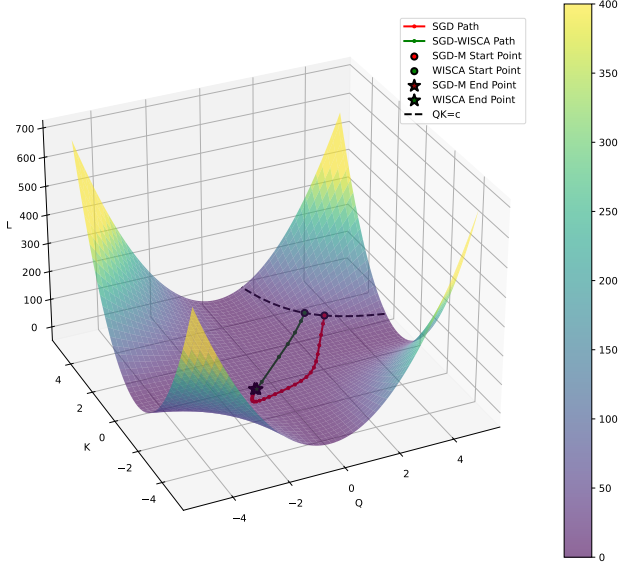


Figure 3: **Comparison of SGD-M (Bottou and Bousquet 2007) and SGD-M-WISCA Optimization Paths.** Red: Optimization trajectory of SGD with momentum ($\beta = 0.9$) starting from a random initialization. Green: Trajectory using WISCA-adjusted initialization ($Q = K$). Both methods minimize $L = (QK - 1)^2$ with learning rate $\eta = 0.01$ and loss threshold $\epsilon = 10^{-2}$. **Observations:** 1. The WISCA path (Green) converges in **7 iterations** with a smooth, flat trajectory, while the random initialization (Red) requires **25 iterations** with oscillatory behavior. 2. All equivalent models on the same contour line ($QK = C$) exhibit slower convergence except at $Q = K$, where the flattest region enables faster stabilization. This demonstrates WISCA’s ability to identify high-quality initializations aligned with flat minima, accelerating convergence without architectural changes.

updating the parameter along the negative gradient direction with learning rate $\eta = \frac{\epsilon}{2(QK-1)}$, the next checkpoint is $(Q - \epsilon K, K - \epsilon Q)$. Now the gradient at this checkpoint is $2((Q - \epsilon K)(K - \epsilon Q) - 1)(K - \epsilon Q, Q - \epsilon K)$. We hope the gradient direction varies as small as possible. Therefore, we have $\frac{Q}{K} = \frac{Q - \epsilon K}{K - \epsilon Q}$ and obtain $K^2 = Q^2$, which means $|Q| = |K|$.

The proposed scaling strategy is also valid for consecutive linear layers, even when activation functions (e.g., ReLU, LeakyReLU (Xu et al. 2015)) are used. Similarly, it is also valid for w_v and w_o in transformer.

To ensure $\|W'_v\|_1 = \|W'_o\|_1$ while preserving the output $\text{Output} = (\text{attention_score} \cdot V) \cdot W_o$, we define:

$$W'_v = W_v \cdot \sqrt{\frac{\|W_o\|_1}{\|W_v\|_1}}, \quad (16)$$

$$W'_o = W_o \cdot \sqrt{\frac{\|W_v\|_1}{\|W_o\|_1}}. \quad (17)$$

In classical Transformer architectures, W_q and W_k typically share the same dimensionality. Under Gaussian initial-

ization, their L_1/L_2 -norms become approximately equal as the parameter count grows, rendering naive WISCA adjustments negligible (Appendix Theorem .3).

Another essential application of WISCA is for the GQA-based architectures (Ainslie et al. 2023) (e.g., g query heads sharing one key/value group), W_q has $g \times$ more parameters than W_k , leading to a significant WISCA scaling ratio of $\sqrt{1/g}$. For GQA, we propose **group-averaged normalization**:

- **Loss Flatness Principle:** For $\mathcal{L} = (QK - 1)^2$, flatness is maximized when $Q = K$.

- **GQA Simulation:**

$$Q = [Q_1, Q_2, \dots, Q_g], \quad K = [K_1, K_1, \dots, K_1], \\ \mathcal{L} = [K_1 \sum_{i=1}^g Q_i - 1]^2.$$

Optimal flatness occurs when $K_1 = \sum_{i=1}^g Q_i$, not $K_1 = Q_1 = Q_2 = \dots = Q_g$.

Conclusion: WISCA adjustments for GQA enforce $\|W_q\|_1 = \|W_k\|_1 \times g$, yielding **larger scaling effects** than in MHA. Similarly, WISCA can be extended to matrix multiplication with unequal matrices, such as the A and B matrices of LoRA.

We have demonstrated both theoretically and empirically that WISCA achieves its goals through core principles in Transformer architecture: Adjust $\|W_q\|_1 = \|W_k\|_1$ and $\|W_v\|_1 = \|W_o\|_1$, while preserving model outputs. The impact of WISCA is more pronounced in architectures with imbalanced parameter groups, such as Grouped Query Attention (GQA), where scaling (e.g., $\sqrt{1/g}$) leads to significant tuning.

In experiments, we implement two WISCA variants:

- **Tensor-wise WISCA:** Global scaling applied to entire weight matrices (Equations 14–17).
- **Channel-wise WISCA:** A finer-grained variant that applies scaling at the channel level, enhancing flexibility in parameter optimization.

Experiments

We designed tensor-wise and channel-wise WISCA for W_q/W_k and W_v/W_o , and conducted pre-training comparative experiments on open-source Llama, Qwen, and popular Mixture-of-Experts (MoE) architectures (Jacobs et al. 1991). The experiments evaluated the training convergence and downstream task performance of different WISCA strategies compared to the original approach. Results demonstrate that WISCA significantly improves model training performance across all tested architectures.

Tensor-wise and Channel-wise WISCA

We implement four WISCA variants targeting different components of the attention mechanism: (1) adjustments on W_q/W_k for attention score computation, covering tensor-wise (Figure 4) and channel-wise (Figure 5) optimizations; and (2) adjustments on W_v/W_o for output projection, also including tensor-wise (Figure 6) and channel-wise (Figure 7) variants.

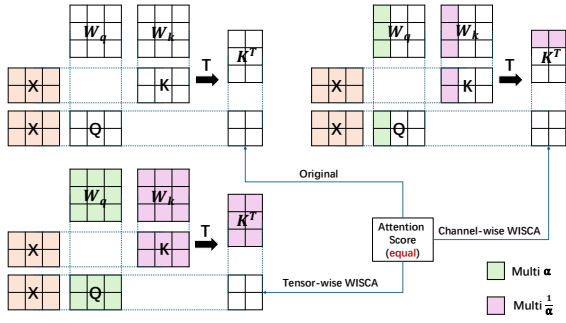


Figure 4: **Comparison of Attention Score Computation Methods.** Original attention mechanism (top-left), tensor-wise WISCA (bottom-down), and channel-wise WISCA (top-right) on W_q/W_k adjustments. All methods produce **identical attention scores** but exhibit **distinct weight patterns**.

As shown in Figure 4, both QK-WISCA variants retain the original attention scores while redistributing weight magnitudes, with channel-wise scaling offering finer-grained control than tensor-wise. Similarly, Figure 6 shows that W_v/W_o adjustments preserve self-attention outputs despite altered weight patterns, mirroring the pattern observed in attention-score optimization.

For Grouped Query Attention (GQA) architectures, we further validate the adaptability of channel-wise WISCA. Figures 5 and 7 demonstrate that GQA’s dimensional asymmetry requires group-aware scaling in channel-wise WISCA.

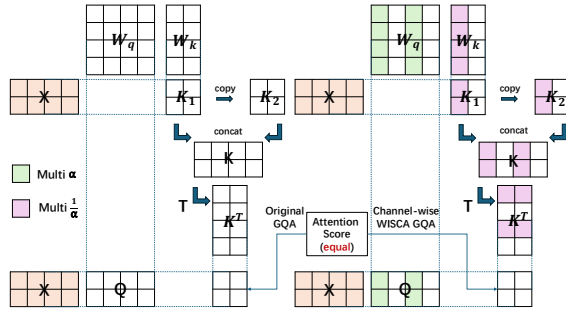


Figure 5: **Channel-wise WISCA in GQA Architecture.** Comparison between original attention (left) and channel-wise WISCA (right) for W_q/W_k adjustments in Grouped Query Attention (GQA). Both methods produce **identical attention scores** but exhibit **distinct weight patterns**. GQA introduces dimensional asymmetry between W_q and W_k , requiring channel-wise WISCA to adapt to group-wise scaling (tensor-wise WISCA remains identical to MHA, omitted here).

Convergence Effect on Mainstream LLMs

To validate WISCA’s effectiveness in real training scenarios, we conduct pre-training experiments on three architectures (**TinyLlama** (Zhang et al. 2024), **Qwen2-1.5B** (Team

2024b), and **Qwen1.5-MoE** (Team 2024a)) using the TinyStories (Eldan and Li 2023) dataset. We compare tensor-wise WISCA strategies (① QK_TEN and ② VO_TEN shown in Figure 4 and Figure 6) against the original training approach, with WISCA applied every 250 iterations while maintaining identical hyperparameters (learning rate, optimizer, batch size, etc.) across all experimental groups. Training loss and test perplexity (PPL) results are summarized in Table 1.

Table 1: Training losses and test PPL scores for different strategies on various models

MODEL	STRATEGY	TRAIN LOSS	TEST PPL
TINYLLAMA	ORIGIN	1.3193	3.78
	① QK_TEN	1.2849	3.66
	② VO_TEN	1.3123	3.75
	①+②	1.2749	3.62
QWEN2-1.5B	ORIGIN	1.355	3.96
	① QK_TEN	1.3417	3.91
	② VO_TEN	1.3507	3.94
	①+②	1.3336	3.88
QWEN1.5-MoE	ORIGIN	1.5497	4.76
	① QK_TEN	1.519	4.62
	② VO_TEN	1.5408	4.72
	①+②	1.5141	4.60

Across all pre-training tasks, the experimental results demonstrate that WISCA consistently improves model convergence behavior. Notably, the combined application of QK-WISCA and VO-WISCA yields superior performance compared to individual module adjustments, exhibiting a **synergistic effect** on the target dataset. This improvement pattern remains consistent across all tested architectures.

Evaluation Results on LLMs

To evaluate WISCA’s zero-shot generalization capabilities, we trained a 1.1B-parameter Llama model from scratch on 1.4B tokens from Wikipedia.en, followed by comprehensive evaluation using the EleutherAI LM Evaluation Harness (Gao et al. 2024).

In the end-to-end evaluation experiments, we validated both tensor/channel-wise WISCA strategies and their four combinatorial variants. Given the pronounced impact of initial WISCA adjustments on model positioning within the loss landscape, we additionally evaluated strategies where WISCA was applied only at initialization (marked as “(init)” in Table 2).

The evaluation experiments demonstrate that combinatorial WISCA strategies (①+③, etc.) significantly outperform individual optimizations, with the best combination achieving a 10.1% average improvement over the baseline (Table 2), highlighting synergistic effects between QK-WISCA and VO-WISCA adjustments.

While initialization-only WISCA retains an average of 97% of the full combinatorial performance, it suggests that periodic adjustments provide incremental refinements

Table 2: Evaluation Metrics of llama-1.1B Trained on 1.4B Tokens from Wikipedia.en. Performance comparison of different attention optimization methods. All metrics seen in table 6

VERSION	BOOLQ↑	ARC-C↑	PIQA↑	WINO↑	AVG↑
ORIGIN	0.3838	0.1741	0.5288	0.5004	0.3968
① QK_TEN	0.3810	0.1843	0.5332	0.4807	0.3948
② QK_ROW	0.3887	0.1817	0.5370	0.5091	0.4041
③ VO_TEN	0.4015	0.1852	0.5294	0.4957	0.4030
④ VO_ROW	0.3817	0.1749	0.5386	0.4988	0.3985
①+③	0.5214	0.1869	0.5413	0.4980	0.4369
②+③	0.4483	0.2014	0.5305	0.5059	0.4215
①+④	0.4226	0.1783	0.5310	0.5075	0.4099
②+④	0.3994	0.1724	0.5430	0.5170	0.4080
①+③(INIT)	0.4703	0.1860	0.5299	0.4964	0.4207
②+③(INIT)	0.3960	0.1792	0.5386	0.5036	0.4044
①+④(INIT)	0.4312	0.1766	0.5308	0.4949	0.4083
②+④(INIT)	0.3917	0.1817	0.5337	0.5043	0.4029

to weight patterns. For resource-constrained scenarios, initialization-only WISCA offers a computationally efficient alternative (no training overhead) while preserving most performance gains.

Table 3: Zero-shot evaluation results on different training steps on llama_moe-5B-A0.8B. All metrics seen in table 7

STEPS (TOKENS)	METRICS AVG↑			PPL(WIKITEXT2)		
	ORIGIN	①+③	+(%)	ORIGIN	①+③	+(%)
1.43B	35.56	37.07	4.25	70.93	68.11	3.98
2.86B	37.88	38.23	0.92	48.17	46.25	3.98
4.29B	39.28	39.49	0.53	40.72	39.17	3.82
5.72B	39.83	40.68	2.13	35.48	34.85	1.77
7.15B	40.13	40.33	0.50	33.29	32.77	1.56
8.58B	40.31	40.69	0.94	31.16	30.80	1.15
10.0B	39.39	40.72	3.38	29.45	29.21	0.82

To analyze WISCA’s impact across training stages, we train a Llama-MoE-5B-A0.8B model for 10B tokens, evaluating seven intermediate checkpoints. Zero-shot performance metrics and perplexity scores are reported in Table 3, demonstrating WISCA’s consistent optimization benefits throughout training.

The results demonstrate that, due to the extensive tuning of WISCA during initialization, the most significant improvements are achieved early in training, when the model’s loss graph smoothness undergoes the largest shift.

While metric fluctuations occur across training steps (e.g., 0.50–3.38% accuracy variations), WISCA consistently outperforms the baseline in all evaluations. The sustained positive trends—particularly the average 1.81% metrics improvement and 2.44% perplexity reduction across 10B tokens—validate its robustness as a general optimization strategy.

Benefits on LoRA

Low-Rank Adaptation (LoRA) (Hu et al. 2022) is a parameter-efficient fine-tuning (PEFT) paradigm widely adopted for large language models (LLMs). The core hypothesis posits that weight updates (ΔW) during model adaptation exhibit a low *intrinsic rank*, implying they can be approximated by low-dimensional structures rather than full-rank matrices.

Given a pre-trained weight matrix $W \in \mathbb{R}^{m \times n}$, LoRA introduces two trainable low-rank matrices $A \in \mathbb{R}^{m \times r}$ and $B \in \mathbb{R}^{r \times n}$, where $r \ll \min(m, n)$. The adapted weight is computed as:

$$W' = W + \Delta W = W + A \cdot B \quad (18)$$

During fine-tuning, *only* A and B are updated, while the original W remains frozen.

When $m \neq n$, the parameter counts of matrices A and B become imbalanced. In standard LoRA, the B matrix is initialized as zero ($\|A\| \neq \|B\|$), enabling dynamic WISCA operations during training. We fine-tuned the DeepSeek-V2-Lite-Chat model on the Alpaca and MetaMath datasets using LoRA, PISSA (Meng, Wang, and Zhang 2024), and RS-LoRA (Kalajdziewski 2023) strategies via Llama-Factory (Zheng et al. 2024), comparing vanilla fine-tuning with WISCA-enhanced training (Table 4). Results validate its universal optimization capability in parameter-efficient fine-tuning (PEFT) scenarios.

The **Alpaca** (Taori et al. 2023) dataset is a widely-used benchmark for instruction tuning, generated by fine-tuning LLaMA on self-instruct-style human-AI interactions to improve language models’ ability to follow diverse commands. **MetaMath** (Yu et al. 2023) is a specialized mathematical reasoning dataset containing 8.4k problem-solution pairs across arithmetic, algebra, and geometry, designed to evaluate and enhance models’ multistep reasoning capabilities.

Table 4: Training Loss Comparison: Vanilla vs. WISCA enhanced SFT fine-tuning for DeepSeek-V2-Lite-Chat (DeepSeek-AI 2024) on Alpaca and MetaMath. All experiments were trained with 3 epochs.

METHOD	ALPACA		METAMATH	
	ORIGIN	WISCA	ORIGIN	WISCA
LoRA	0.8602	0.8532	0.0779	0.0770
PISSA	0.6227	0.6176	0.0692	0.0688
RS-LoRA	0.6773	0.6760	0.0744	0.0726

Since the B matrix in vanilla LoRA is initialized as a zero matrix, WISCA cannot be applied during initialization. In our experiments (Table 4), WISCA operations were performed at one-third of the total training iterations.

Benefits on Eagle

EAGLE (Li et al. 2024) is a state-of-the-art speculative sampling framework that significantly accelerates LLMs’ inference. It employs a draft model (typically a small neural network) to generate candidate token sequences, which are then validated in parallel by the target LLM.

We implement EAGLE by training a draft model for **LLaMA 3.1 Instruct 8B** (Grattafiori et al. 2024). The draft model architecture consists of a single Transformer layer with self-attention, incorporating our proposed WISCA strategy during training to optimize weight patterns.

Dataset: We use the **ShareGPT** dataset, a collection of 90K high-quality human-AI conversations spanning diverse domains (e.g., coding, reasoning, open-ended dialogue). Each example contains multi-turn interactions, making it suitable for training instruction-following draft models.

Table 5: EAGLE-1 Performance: Average Accepted Tokens and Training Metrics. Tree/Chain modes use depth=6/top-k=10 and depth=5, respectively.

METRIC	ORIGINAL		WISCA	
	TREE	CHAIN	TREE	CHAIN
MT-BENCH	3.001	1.528	3.009	1.593
GSM8K	3.234	1.818	3.271	1.809
HUMAN-EVAL	3.708	2.103	3.715	2.110
ALPACA-EVAL	2.874	1.462	2.900	1.478
TRAIN LOSS	0.7168		0.7113	
VAL LOSS	0.7359		0.7312	
TRAIN ACC (%)	79.28		79.49	
VAL ACC (%)	77.03		77.11	

In experiments with the EAGLE draft model (Table 5), we applied tensor-wise WISCA to the $[w_q, w_k]$ and $[w_v, w_o]$ modules. The results show that WISCA consistently improves training efficiency, with the WISCA-enhanced model outperforming the baseline in end-to-end evaluations in both *tree* and *chain* generation modes. This validates the generalizability of WISCA’s weight pattern optimization in speculative sampling frameworks.

Related Work

Loss Landscape Optimization. Sharpness-Aware Minimization (SAM) (Foret et al. 2020) explicitly minimizes loss sharpness, albeit at the cost of approximately double the computation per parameter update. Stochastic Weight Averaging (SWA) (Izmailov et al. 2018) improves generalization by weight averaging, but requires extensive training. WISCA implicitly smooths the loss landscape through weight pattern adjustments, achieving efficiency gains with minimal overhead.

Weight Balancing and Normalization. Query key normalization (QKN) (Henry et al. 2020) improves the stability of transformer training by applying L2 normalization to the query (Q) and key (K) matrices, transforming their dot products into cosine similarities. Weight normalization (Salimans and Kingma 2016) reparameterizes weights to decouple direction and magnitude. Unlike these methods, WISCA enforces *functional equivalence* while balancing weight norms, enabling dynamic transitions between equivalent models without architectural changes.

Model Equivalence and Weight Patterns. The Lottery ticket hypothesis (Frankle and Carbin 2018) identifies performant sparse subnets, whereas permutation symmetry re-

veals equivalence under weight permutations. WISCA leverages these insights to navigate the loss landscape via equivalent model transitions, prioritizing flat minima for enhanced generalization.

Parameter-Efficient Fine-Tuning (PEFT). Low-Rank Adaptation (LoRA) (Hu et al. 2022) reduces trainable parameters by decomposing weight updates into low-rank matrices. Recent variants like PiSSA (Meng, Wang, and Zhang 2024) further improve efficiency by adapting only the principal singular values and vectors of the weight matrices, achieving faster convergence than LoRA. WISCA can be integrated with PEFT methods such as LoRA and PiSSA to optimize weight patterns in their low-rank matrices, enhancing both training stability and task-specific adaptation without introducing additional parameters.

Speculative Decoding. EAGLE (Li et al. 2024) accelerates LLM inference through a small draft model. Our work improves EAGLE by applying WISCA to the draft layer training, improving token acceptance rates through better weight patterns.

Conclusion

In this work, we introduced WISCA, a novel training optimization strategy that leverages equivalent model transitions to reshape weight patterns while maintaining functional equivalence. Our theoretical analysis established a fundamental connection between weight pattern smoothness and generalization performance, demonstrating that flatter minima achieved through the dynamic tuning of WISCA lead to superior model robustness. The proposed method operates without architectural modifications, instead optimizing the training trajectory by strategically transitioning between equivalent models with improved weight configurations. Extensive experiments across diverse architectures—including GQA, MoE, and PEFT frameworks like LoRA—validated WISCA’s broad applicability and effectiveness. Key findings include:

- **Pretraining Efficiency:** WISCA reduced training perplexity by 2.12% and improved zero-shot task performance by 5.6% on average, with particularly pronounced gains in GQA architectures due to their inherent parameter imbalance.
- **Fine-Tuning Robustness:** Integration with LoRA and PiSSA yielded consistent training loss reductions, highlighting WISCA’s compatibility with parameter-efficient adaptation.
- **Inference Acceleration:** When applied to EAGLE’s draft model, WISCA increased token acceptance rates in both tree and chain modes, underscoring its utility in speculative decoding.

This paper proposes a weight scaling method for self-attention modules and LoRA to achieve a flatter equivalent model. In the future, we can explore more strategies for finding equivalent models and more strategies for judging the convergence of equivalent models. And not only in the field of LLMs, but also in other fields, more suitable equivalent model strategies can be designed for different neural networks.

References

- Ainslie, J.; Lee-Thorp, J.; De Jong, M.; Zemlyanskiy, Y.; Lebrón, F.; and Sanghai, S. 2023. Gqa: Training generalized multi-query transformer models from multi-head checkpoints. *arXiv preprint arXiv:2305.13245*.
- Barron, A. 1993. Universal approximation bounds for superpositions of a sigmoidal function. *IEEE Transactions on Information Theory*, 39(3): 930–945.
- Bisk, Y.; Zellers, R.; Bras, R. L.; Gao, J.; and Choi, Y. 2020. PIQA: Reasoning about Physical Commonsense in Natural Language. In *Thirty-Fourth AAAI Conference on Artificial Intelligence*.
- Bottou, L.; and Bousquet, O. 2007. The tradeoffs of large scale learning. *Advances in neural information processing systems*, 20.
- Chen, M.; Tworek, J.; Jun, H.; Yuan, Q.; Pinto, H. P. D. O.; Kaplan, J.; Edwards, H.; Burda, Y.; Joseph, N.; Brockman, G.; et al. 2021. Evaluating large language models trained on code. *arXiv preprint arXiv:2107.03374*.
- Clark, C.; Lee, K.; Chang, M.-W.; Kwiatkowski, T.; Collins, M.; and Toutanova, K. 2019. Boolq: Exploring the surprising difficulty of natural yes/no questions. *arXiv preprint arXiv:1905.10044*.
- Clark, P.; Cowhey, I.; Etzioni, O.; Khot, T.; Sabharwal, A.; Schoenick, C.; and Tafford, O. 2018. Think you have Solved Question Answering? Try ARC, the AI2 Reasoning Challenge. *arXiv:1803.05457v1*.
- Cobbe, K.; Kosaraju, V.; Bavarian, M.; Chen, M.; Jun, H.; Kaiser, L.; Plappert, M.; Tworek, J.; Hilton, J.; Nakano, R.; et al. 2021. Training verifiers to solve math word problems, 2021. URL <https://arxiv.org/abs/2110.14168>, 9.
- DeepSeek-AI. 2024. DeepSeek-V2: A Strong, Economical, and Efficient Mixture-of-Experts Language Model. *arXiv:2405.04434*.
- Eldan, R.; and Li, Y. 2023. Tinystories: How small can language models be and still speak coherent english? *arXiv preprint arXiv:2305.07759*.
- Foret, P.; Kleiner, A.; Mobahi, H.; and Neyshabur, B. 2020. Sharpness-aware minimization for efficiently improving generalization. *arXiv preprint arXiv:2010.01412*.
- Frankle, J.; and Carbin, M. 2018. The lottery ticket hypothesis: Finding sparse, trainable neural networks. *arXiv preprint arXiv:1803.03635*.
- Gao, L.; Tow, J.; Abbasi, B.; Biderman, S.; Black, S.; DiPofi, A.; Foster, C.; Golding, L.; Hsu, J.; Le Noac’h, A.; Li, H.; McDonell, K.; Muennighoff, N.; Ociepa, C.; Phang, J.; Reynolds, L.; Schoelkopf, H.; Skowron, A.; Sutawika, L.; Tang, E.; Thite, A.; Wang, B.; Wang, K.; and Zou, A. 2024. The Language Model Evaluation Harness.
- Grattafiori, A.; Dubey, A.; Jauhri, A.; Pandey, A.; Kadian, A.; Al-Dahle, A.; Letman, A.; Mathur, A.; Schelten, A.; Vaughan, A.; et al. 2024. The llama 3 herd of models. *arXiv preprint arXiv:2407.21783*.
- Henry, A.; Dachapally, P. R.; Pawar, S.; and Chen, Y. 2020. Query-key normalization for transformers. *arXiv preprint arXiv:2010.04245*.
- Hu, E. J.; Shen, Y.; Wallis, P.; Allen-Zhu, Z.; Li, Y.; Wang, S.; Wang, L.; Chen, W.; et al. 2022. Lora: Low-rank adaptation of large language models. *ICLR*, 1(2): 3.
- Huang, Y.; Bai, Y.; Zhu, Z.; Zhang, J.; Zhang, J.; Su, T.; Liu, J.; Lv, C.; Zhang, Y.; Lei, J.; Fu, Y.; Sun, M.; and He, J. 2023. C-Eval: A Multi-Level Multi-Discipline Chinese Evaluation Suite for Foundation Models. *arXiv preprint arXiv:2305.08322*.
- Huo, F.; Tan, J.; Zhang, K.; Cai, X.; and Sun, S. 2025. C2T: A Classifier-Based Tree Construction Method in Speculative Decoding. *arXiv preprint arXiv:2502.13652*.
- Izmailov, P.; Podoprikin, D.; Garipov, T.; Vetrov, D.; and Wilson, A. G. 2018. Averaging weights leads to wider optima and better generalization. *arXiv preprint arXiv:1803.05407*.
- Jacobs, R. A.; Jordan, M. I.; Nowlan, S. J.; and Hinton, G. E. 1991. Adaptive mixtures of local experts. *Neural computation*, 3(1): 79–87.
- Kalajdziewski, D. 2023. A rank stabilization scaling factor for fine-tuning with lora. *arXiv preprint arXiv:2312.03732*.
- Keskar, N. S.; Mudigere, D.; Nocedal, J.; Smelyanskiy, M.; and Tang, P. T. P. 2016. On large-batch training for deep learning: Generalization gap and sharp minima. *arXiv preprint arXiv:1609.04836*.
- LeCun, Y.; Bottou, L.; Bengio, Y.; and Haffner, P. 2002. Gradient-based learning applied to document recognition. *Proceedings of the IEEE*, 86(11): 2278–2324.
- Leviathan, Y.; Kalman, M.; and Matias, Y. 2023. Fast inference from transformers via speculative decoding. In *International Conference on Machine Learning*, 19274–19286. PMLR.
- Li, Y.; Wei, F.; Zhang, C.; and Zhang, H. 2024. Eagle: Speculative sampling requires rethinking feature uncertainty. *arXiv preprint arXiv:2401.15077*.
- Meng, F.; Wang, Z.; and Zhang, M. 2024. Pissa: Principal singular values and singular vectors adaptation of large language models. *Advances in Neural Information Processing Systems*, 37: 121038–121072.
- Merity, S.; Xiong, C.; Bradbury, J.; and Socher, R. 2016. Pointer Sentinel Mixture Models. *arXiv:1609.07843*.
- Mihaylov, T.; Clark, P.; Khot, T.; and Sabharwal, A. 2018. Can a Suit of Armor Conduct Electricity? A New Dataset for Open Book Question Answering. In *EMNLP*.
- Qin, J.; Tan, J.; Zhang, K.; Cai, X.; and Wang, W. 2025. MaskPrune: Mask-based LLM Pruning for Layer-wise Uniform Structures. *arXiv preprint arXiv:2502.14008*.
- Salimans, T.; and Kingma, D. P. 2016. Weight normalization: A simple reparameterization to accelerate training of deep neural networks. *Advances in neural information processing systems*, 29.
- Shazeer, N. 2019. Fast transformer decoding: One write-head is all you need. *arXiv preprint arXiv:1911.02150*.
- Taori, R.; Gulrajani, I.; Zhang, T.; Dubois, Y.; Li, X.; Guestrin, C.; Liang, P.; and Hashimoto, T. B. 2023. Stanford Alpaca: An Instruction-following LLaMA model. https://github.com/tatsu-lab/stanford_alpaca.

Team, Q. 2024a. Qwen1.5-MoE: Matching 7B Model Performance with 1/3 Activated Parameters”.

Team, Q. 2024b. Qwen2 technical report. *arXiv preprint arXiv:2412.15115*.

Thrush, T.; Jiang, R.; Bartolo, M.; Singh, A.; Williams, A.; Kiela, D.; and Ross, C. 2022. Winoground: Probing vision and language models for visio-linguistic compositionality. In *CVPR*.

Touvron, H.; Lavril, T.; Izacard, G.; Martinet, X.; Lachaux, M.-A.; Lacroix, T.; Rozière, B.; Goyal, N.; Hambro, E.; Azhar, F.; et al. 2023. Llama: Open and efficient foundation language models. *arXiv preprint arXiv:2302.13971*.

Vaswani, A.; Shazeer, N.; Parmar, N.; Uszkoreit, J.; Jones, L.; Gomez, A. N.; Kaiser, Ł.; and Polosukhin, I. 2017. Attention is all you need. *Advances in neural information processing systems*, 30.

Xu, B.; Wang, N.; Chen, T.; and Li, M. 2015. Empirical evaluation of rectified activations in convolutional network. *arXiv preprint arXiv:1505.00853*.

Xu, L.; Xie, H.; Qin, S.-Z. J.; Tao, X.; and Wang, F. L. 2023. Parameter-efficient fine-tuning methods for pretrained language models: A critical review and assessment. *arXiv preprint arXiv:2312.12148*.

Yu, L.; Jiang, W.; Shi, H.; Yu, J.; Liu, Z.; Zhang, Y.; Kwok, J. T.; Li, Z.; Weller, A.; and Liu, W. 2023. Metamath: Bootstrap your own mathematical questions for large language models. *arXiv preprint arXiv:2309.12284*.

Zellers, R.; Holtzman, A.; Bisk, Y.; Farhadi, A.; and Choi, Y. 2019. HellaSwag: Can a Machine Really Finish Your Sentence? In *Proceedings of the 57th Annual Meeting of the Association for Computational Linguistics*.

Zhang, P.; Zeng, G.; Wang, T.; and Lu, W. 2024. TinyLlama: An Open-Source Small Language Model. *arXiv:2401.02385*.

Zheng, L.; Chiang, W.-L.; Sheng, Y.; Zhuang, S.; Wu, Z.; Zhuang, Y.; Lin, Z.; Li, Z.; Li, D.; Xing, E.; et al. 2023. Judging llm-as-a-judge with mt-bench and chatbot arena. *Advances in Neural Information Processing Systems*, 36: 46595–46623.

Zheng, Y.; Zhang, R.; Zhang, J.; Ye, Y.; Luo, Z.; Feng, Z.; and Ma, Y. 2024. LlamaFactory: Unified Efficient Fine-Tuning of 100+ Language Models. In *Proceedings of the 62nd Annual Meeting of the Association for Computational Linguistics (Volume 3: System Demonstrations)*. Bangkok, Thailand: Association for Computational Linguistics.

Appendix

Norm Convergence in Classical Transformers

Theorem 3. For Gaussian-initialized matrices $\mathbf{W}_q, \mathbf{W}_k \in \mathbb{R}^{m \times n}$ with i.i.d. entries $\mathcal{N}(0, \sigma^2)$, the L_1 - and L_2 -norms satisfy:

$$\frac{\|\mathbf{W}_q\|_1}{\|\mathbf{W}_k\|_1} \xrightarrow{p} 1 \quad \text{and} \quad \frac{\|\mathbf{W}_q\|_2}{\|\mathbf{W}_k\|_2} \xrightarrow{p} 1 \quad \text{as } mn \rightarrow \infty,$$

where \xrightarrow{p} denotes convergence in probability.

Proof. 1. **L_2 -Norm (Frobenius Norm):** Let $\|\mathbf{W}\|_2^2 = \sum_{i,j} W_{ij}^2$. For Gaussian entries:

$$\mathbb{E}[\|\mathbf{W}\|_2^2] = mn\sigma^2, \quad \text{Var}(\|\mathbf{W}\|_2^2) = 2mn\sigma^4.$$

By Chebyshev's inequality:

$$P\left(\left|\frac{\|\mathbf{W}\|_2^2}{mn\sigma^2} - 1\right| > \epsilon\right) \leq \frac{2mn\sigma^4}{(mn\sigma^2\epsilon)^2} = \frac{2}{\epsilon^2 mn} \rightarrow 0.$$

Thus, $\|\mathbf{W}_q\|_2 / \|\mathbf{W}_k\|_2 \rightarrow 1$.

2. **L_1 -Norm:** Let $\|\mathbf{W}\|_1 = \sum_{i,j} |W_{ij}|$. For $W_{ij} \sim \mathcal{N}(0, \sigma^2)$:

$$\mathbb{E}[|W_{ij}|] = \sigma\sqrt{\frac{2}{\pi}}, \quad \text{Var}(|W_{ij}|) = \sigma^2\left(1 - \frac{2}{\pi}\right).$$

Summing over mn terms:

$$\mathbb{E}[\|\mathbf{W}\|_1] = mn\sigma\sqrt{\frac{2}{\pi}}, \quad \text{Var}(\|\mathbf{W}\|_1) = mn\sigma^2\left(1 - \frac{2}{\pi}\right).$$

Again by Chebyshev:

$$P\left(\left|\frac{\|\mathbf{W}\|_1}{mn\sigma\sqrt{2/\pi}} - 1\right| > \epsilon\right) \leq \frac{1 - 2/\pi}{\epsilon^2 mn} \rightarrow 0.$$

Hence, $\|\mathbf{W}_q\|_1 / \|\mathbf{W}_k\|_1 \rightarrow 1$. \square

Appendix figures

In this Appendix, we present the WISCA strategy for the w_v and w_o components of the transformer block, which were not exhibited in the main text. Figure 6 illustrates the matrix perspective of tensor-wise WISCA and channel-wise WISCA for a general attention module. Similarly, Figure 7 provides a schematic representation for the attention module with GQA.

Summary of All Metrics

In the experimental section, we conducted pre-training tasks using the tinylama and llama-moe models. While the main text includes a streamlined table focusing on zero-shot evaluation metrics, this appendix provides a complete overview of all evaluation metrics for thorough analysis.

The following tables provide detailed metrics gathered from our comprehensive evaluations. Table 6 breaks down the individual performance metrics across various tests, highlighting the comparative effectiveness of different attention optimization strategies applied to the Llama model. We additionally explore the impact of WISCA at various stages

of training in Table 7, showcasing the zero-shot evaluation results for the llama-moe-5B-A0.8B model across different checkpoints and training steps.

These results underscore the efficacy of our approaches. By presenting all metrics here, we aim to furnish a deeper understanding of the evaluation outcomes in the context of our experimental framework.

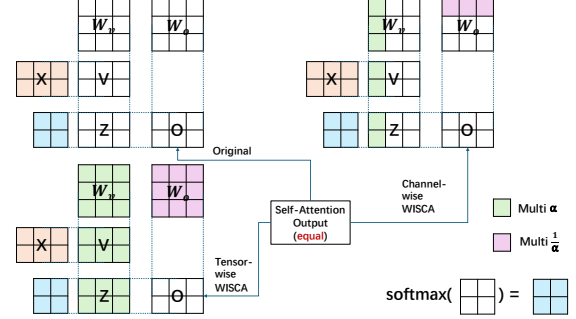


Figure 6: **Comparison of Output Projection Methods.** Original output projection (left), tensor-wise WISCA (middle), and channel-wise WISCA (right) on W_v/W_o adjustments. All methods produce **identical self-attention outputs** but exhibit **distinct weight patterns**.

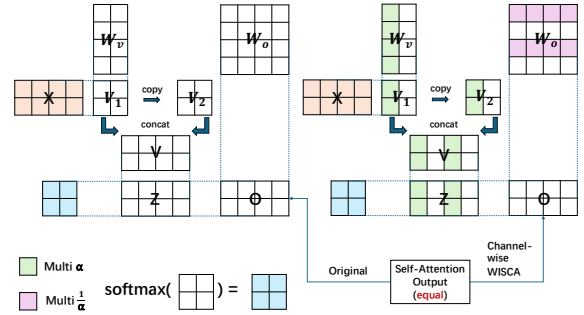


Figure 7: **Channel-wise WISCA for Output Projection in GQA.** Comparison between original output projection (left) and channel-wise WISCA (right) on W_v/W_o in Grouped Query Attention (GQA). Both methods yield **identical self-attention outputs** but with **distinct weight patterns**. GQA's dimensional asymmetry requires channel-wise WISCA to adapt group-aware scaling, while tensor-wise WISCA remains equivalent to MHA (omitted here).

Proof of Convergence

Why does the convergence become stable after using WISCA? Here is an intuitive explanation. Considering the landscape $f(Q, K) = (QK - 1)^2$ and the current checkpoint is (Q, K) , the gradient is $2(QK - 1)(K, Q)$. After updating the parameter along the negative gradient direction with learning rate $\eta = \frac{\epsilon}{2(QK - 1)}$, the next checkpoint is $(Q - \epsilon K, K - \epsilon Q)$. Now the gradient at this checkpoint is $2((Q - \epsilon K)(K - \epsilon Q) - 1)(K - \epsilon Q, Q - \epsilon K)$. We hope the gradient direction varies as small as possible. Therefore, we have $\frac{Q}{K} = \frac{Q - \epsilon K}{K - \epsilon Q}$ and obtain $K^2 = Q^2$, which means $|Q| = |K|$.

Table 6: All metrics of table2

VERSION	BOOLQ↑	ARC-C↑	ARC-E↑	PIQA↑	WINO↑	HELLAS↑	OBQA↑	CEVAL↑	AVG↑
ORIGIN	0.3838	0.1741	0.3274	0.5288	0.5004	0.2650	0.1300	0.2437	0.3192
① QK_TEN	0.3810	0.1843	0.3228	0.5332	0.4807	0.2617	0.1280	0.2511	0.3179
② QK_ROW	0.3887	0.1817	0.3102	0.5370	0.5091	0.2617	0.1280	0.2533	0.3212
③ VO_TEN	0.4015	0.1852	0.3081	0.5294	0.4957	0.2653	0.1380	0.2585	0.3227
④ VO_ROW	0.3817	0.1749	0.3178	0.5386	0.4988	0.2629	0.1500	0.2548	0.3224
①+③	0.5214	0.1869	0.3165	0.5413	0.4980	0.2634	0.1340	0.2585	0.3400
②+③	0.4483	0.2014	0.3165	0.5305	0.5059	0.2656	0.1320	0.2578	0.3323
①+④	0.4226	0.1783	0.3199	0.5310	0.5075	0.2645	0.1260	0.2377	0.3234
②+④	0.3994	0.1724	0.3224	0.5430	0.5170	0.2621	0.1340	0.2377	0.3235
①+③(INIT)	0.4703	0.1860	0.3182	0.5299	0.4964	0.2637	0.1300	0.2623	0.3321
②+③(INIT)	0.3960	0.1792	0.3207	0.5386	0.5036	0.2652	0.1120	0.2355	0.3189
①+④(INIT)	0.4312	0.1766	0.3203	0.5308	0.4949	0.2644	0.1220	0.2541	0.3243
②+④(INIT)	0.3917	0.1817	0.3199	0.5337	0.5043	0.2631	0.1240	0.2311	0.3187

Table 7: Zero-shot evaluation results on different training steps on llama_moe-5B-A0.8B.

METRIC	1w	2w	3w	4w	5w	6w	7w
TRAINED TOKENS	1.43B	2.86B	4.29B	5.72B	7.15B	8.58B	10B
<i>Baseline</i>							
ARC-C	19.28	18.69	17.66	19.11	20.22	19.20	20.73
ARC-E	32.74	37.54	41.33	42.80	43.43	43.56	44.57
BOOLQ	48.10	60.06	60.55	62.05	61.13	61.07	49.36
H-SWAG	26.80	27.32	27.86	28.47	28.97	29.44	29.84
OPENBQ	11.80	12.80	13.80	13.40	14.00	16.00	15.60
PIQA	57.73	58.60	60.39	61.53	62.40	63.11	62.89
WINO	52.49	50.12	53.35	51.46	50.75	49.80	52.72
AVG	35.56	37.88	39.28	39.83	40.13	40.31	39.39
PPL(WIKITEXT2)	70.93	48.17	40.72	35.48	33.29	31.16	29.45
<i>QK</i>							
ARC-C	18.26	18.43	18.60	17.83	18.77	18.34	20.22
ARC-E	33.00	37.58	39.86	42.68	44.19	45.29	44.78
BOOLQ	49.11	62.23	62.08	62.17	61.87	61.80	61.41
H-SWAG	26.65	27.34	28.17	28.57	28.95	29.43	29.74
OPENBQ	12.00	14.00	14.60	15.00	16.00	15.00	14.60
PIQA	57.13	59.63	60.88	62.35	63.00	63.66	64.31
WINO	50.67	52.41	50.75	51.85	50.51	52.88	52.49
AVG	35.26	38.80	39.28	40.06	40.47	40.91	41.08
METRIC.GAIN(%)	-0.84	+2.43	0.00	+0.58	+0.85	+1.49	+4.29
PPL(WIKITEXT2)	69.44	47.12	39.74	34.97	32.86	30.99	29.19
PPL.GAIN(%)	+2.10	+2.19	+2.42	+1.43	+1.29	+0.54	+0.85
<i>QKVO</i>							
ARC-C	17.58	18.60	18.09	19.97	18.77	20.39	18.77
ARC-E	35.40	38.22	40.74	43.77	43.94	44.82	44.19
BOOLQ	60.70	61.80	60.09	61.74	61.68	61.80	59.79
H-SWAG	26.75	27.49	28.12	28.69	28.89	29.40	29.89
OPENBQ	11.40	13.00	16.40	15.60	16.40	15.40	17.80
PIQA	58.38	59.41	61.26	62.68	62.62	63.11	63.60
WINO	49.25	49.09	51.70	52.33	50.04	49.88	50.99
AVG	37.07	38.23	39.49	40.68	40.33	40.69	40.72
METRIC.GAIN(%)	+4.25	+0.92	+0.53	+2.13	+0.50	+0.94	+3.38
PPL(WIKITEXT2)	68.11	46.25	39.17	34.85	32.77	30.80	29.21
PPL.GAIN(%)	+3.98	+3.98	+3.82	+1.77	+1.56	+1.15	+0.82